Electron Capture and Loss Cross Sections for Protons Passing through Air

H. KANNER
Department of Physics and Institute for Nuclear Studies, University of Chicago, Chicago, Illinois
(Received August 31, 1951)

Measurements have been made of the electron-loss cross section σ_1 and the electron-capture cross section σ_c for hydrogen beams in air. σ_1 varied from 24.4×10^{-17} cm^2 at 40.8 kv to 13.6×10^{-17} cm^2 at 325 kv. σ_c varied from 20.8×10^{-17} cm^2 at 31.4 kv to 2.7×10^{-17} cm^2 at 122 kv. In the ranges quoted, the cross sections were well represented by the formulas,

$$\sigma_1=(24.54-0.866E/E_0)\times10^{-17}\text{ cm}^2,\quad \sigma_c=[41.1\exp(-0.562E/E_0)]\times10^{-17}\text{ cm}^2,$$

where $E_0=24.8$ kv, the energy of a proton having the velocity $e^2/\hbar$. By extrapolation of the data, σ_1 was found to equal σ_c at energy E_0.

I. INTRODUCTION

A KNOWLEDGE of the cross sections for electron capture and loss by light ions is a valuable aid to the understanding of the energy loss of these particles in matter, particularly at the low energy end of their range where charge exchanges are numerous. This is true for two reasons: (1) The rate of energy loss by ionization is dependent on the average charge of the particle, a quantity directly determined by the ratio of the capture and loss cross sections; and (2) a capture event followed by a loss event is equivalent to a simple ionizing encounter, and must in itself produce at least as great an energy loss as the latter.

The earlier work on this subject was performed using low energy canal rays,[1–5] or high-energy alpha particles from radioactive sources.[6–8] Recent measurements on proton beams of energies from 20 to 400 kv have been made by Hall,[9] who determined the ratio of the capture and loss cross sections in several metals; Montague,[10] who measured the loss cross section in hydrogen gas; and Ribe,[11] who measured both the capture cross section and the ratio of the capture and loss cross sections in hydrogen. The present work concerns itself with the capture and loss cross sections for protons in air, using essentially the methods and arrangement of apparatus of Montague and Ribe.

The procedure was to direct a proton beam at a thin nitrocellulose window. As a result of charge exchange processes in the window, the emergent beam contained a component of neutral hydrogen atoms as well as protons. A uniform magnetic field in the region beyond the window separated the charged and neutral components, each eventually entering a detecting device. When controlled pressures of air were admitted to the region between the window and the detectors, consequent electron exchanges between the beam particles and air atoms caused a diminution, with increasing air pressure, in the observed intensity at the two detectors. Making the assumption, to be examined critically below, that any change of charge suffered by a beam particle alters its trajectory to the extent that it can no longer enter its respective detector, the dependence of observed intensity on pressure is given by $\exp(-N\sigma d)$, where N is the number of gas atoms per cubic centimeter, d is the total path length in the gas-containing region, and σ is the cross section for the process under observation.

II. DESCRIPTION OF APPARATUS

The initial proton beam was produced by the University of Chicago 400-kv Cockroft-Walton accelerator (kevatron) described elsehwere.[12] A selecting magnet separated the proton beam from the molecular ions. The protons then passed through a collimating assembly consisting of two circular apertures 1.58 mm in diameter and 86 cm apart. After passing through an insulated wire gauze for monitoring purposes, the beam impinged on a nitrocellulose "zapon" window, which was aluminized to prevent its retaining an electrostatic charge.

It should be mentioned at this point that in the low energy work (<80 kv) the molecular ion beam was used. On striking the window, the ions would break up, yielding protons of half the energy of the ions. This procedure was necessary because of the failure of the kevatron to produce a well-focused beam at low voltages.

The window provided the entrance to the deflection chamber, described more fully in previous papers,[10,11] which was situated between the poles of an electromagnet, the pole pieces of which were 12.7 cm in diameter and 3.17 cm apart. The two detectors used in the work were located as follows: (1) diametrically opposite to the window, corresponding to no deflection of the initial beam; and (2) in a position corresponding to a 60 degree deflection of the initial beam. These will henceforth be called the 0° and 60° positions, respec-

[1] E. Ruchardt, Ann. Physik **71**, 377 (1923).
[2] A. Ruttenauer, Z. Physik **4**, 267 (1921).
[3] H. Bartels, Ann. Physik **6**, 957 (1930).
[4] H. Bartels, Ann. Physik **13**, 373 (1932).
[5] P. Rudnick, Phys. Rev. **38**, 1342 (1931).
[6] E. Rutherford, Phil. Mag. **47**, 277 (1924).
[7] P. Kapitza, Proc. Roy. Soc. (London) **106**, 602 (1924).
[8] G. H. Henderson, Proc. Roy. Soc. (London) **114**, 241 (1927).
[9] T. Hall, Phys. Rev. **79**, 504 (1950).
[10] J. H. Montague, Phys. Rev. **81**, 1026 (1951).
[11] F. L. Ribe, Phys. Rev. **84**, 1217 (1951).
[12] Allison, del Rosario, Hinton, and Wilcox, Phys. Rev. **71**, 139 (1947).

tively. The detectors themselves were of two kinds. One was simply a faraday cage behind an entrance slit; the other, which will henceforth be called the "Montague detector," consisted of a plate of beryllium-copper at a slight inclination to the beam and maintained at a negative potential of $67\frac{1}{2}$ volts relative to ground. The entrance slits of both detectors, as well as the Zapon window, were tangent to the cylinder defined by the magnet poles.

Since the faraday cage was always kept within 0.2 volt of ground potential and was in the stray field of the magnet, any secondary electrons emitted from its walls were unable to escape. As a consequence, the faraday cage had zero response to neutral particles. The Montague detector, on the other hand, was specifically designed to collect the secondary electrons emitted from the beryllium-copper plate. By virtue of the near parallelism of the electric and magnetic fields, the sensitivity of the Montague detector was found to be independent of the magnetic field strength, and, within the limits of experimental error, was the same for neutral and charged particles. (The term "sensitivity" as used above and elsewhere in this paper shall be taken to mean the charge collected by a detector per particle entering it.)

The currents from the monitor and the detector in use were amplified by direct-current amplifiers,[13] and finally read as galvanometer deflections. In the usual procedure, a 100 megohm input grid resistor was used for the monitor current and a 1000 megohm one for the detector current. The amplifier gains could be conveniently varied by means of 1000K decade resistor boxes in series with the galvanometers.

A generating fluxmeter, whose armature projected into a can sealed in the chamber wall, served to provide readings of the relative magnetic field strength. This instrument was too inaccurate to be used for quantitative measurements; its principal use was to indicate when zero field had been attained after multiple reversals of the magnet current. By always following the procedure of first zeroing the magnet and then adjusting the magnet current in the direction of increasing current, a one-to-one relationship between magnet current and field strength was maintained.

The air used in the measurements was freed of CO_2 and moisture by passing it through a 3-ft-long drying tube containing, in one-foot sections, KOH pellets, "Dryerite," and finally glass beads dusted with P_2O_5. The air was admitted via this tube to a one-liter storage bulb at rates not exceeding 0.014 cm^3 per minute. From the storage bulb the air could be admitted to the electron-exchange chamber by means of a needle valve, a method which gave adequate control since the pressure in the storage bulb was usually held at about 0.1 mm. The chamber pressures were measured with a McLeod gauge. During the measurements at "zero" pressure, the chamber was directly opened to a vacuum system, with a resulting chamber pressure that was always less than 10^{-4} mm.

[13] The circuit is given on the data sheet for the Raytheon CK5697/CK570 electrometer triode, published by the Raytheon Mfg. Co., Newton, Mass.

III. EXPERIMNETAL PROCEDURE

A. Cross-Section Measurement

All data were taken by simultaneous readings of the detector and monitor galvanometers. For brevity, the ratio of the detector and monitor galvanometer deflections will henceforth be termed r, the detector response. To minimize the effects of amplifier drift, the zero readings of these galvanometers were frequently taken, as will be described below. This was simply accomplished by turning off the current to the selecting magnet, so that no beam could enter the apparatus. In normal operation, the faraday cage was at the 60° position and the Montague detector at the 0° position. Both had their entrance slits set to about 1 mm.

The energy of the beam after penetrating the window was measured by taking a profile of the 60° detector response as a function of magnet current, the previously-mentioned precautions of first zeroing the magnet and then only increasing the magnet current being observed. During this energy measurement, the chamber would be open to the vacuum system. The zero readings of the two galvanometers were taken immediately before and after the profile readings. If the two sets of zero readings differed due to drift, a linear interpolation was used to obtain an assumed zero for each profile point.

A measurement of a capture or loss cross section would now be made, much of the procedure being common to both. In the case of the capture measurement, the faraday cage was used at the 60° position. The magnet was carefully zeroed and then set exactly to the field corresponding to the peak of the previously-obtained profile. For the loss measurements, the Montague detector was used at the 0° position and the magnet would usually be set approximately to the peaking field to obtain the standard radius of curvature of 11 cm for protons, but in some of the runs the magnet current was adjusted to obtain smaller radii of curvature.

The following procedure was used for either cross section: The desired pressure of air was admitted to the chamber, the McLeod gauge was read, and zero readings of the galvanometers were taken. Immediately following the last step, the selecting magnet current was rapidly adjusted to aim the kevatron beam at the window, and a minimum of three simultaneous detector *versus* monitor readings were taken. The chamber was now opened to the vacuum system after first trapping the gas in the McLeod gauge bulb for a second pressure reading. As soon as the chamber was fully pumped out, as indicated by an ionization gauge in the vacuum system, three or more detector and monitor readings were again taken, after which the selecting magnet

would be turned off and a second set of zero readings taken. The time required for pumping out was never over 20 seconds. This process, at a given beam energy, was repeated using from three to six pressure values.

B. Magnet Calibration

The magnet was calibrated by taking profiles of magnet current against 60° detector response at known beam energies with the Zapon window removed. The profiles were sufficiently sharp under these conditions (broadening due to scattering at the window eliminated) that it was necessary only to peak the detector galvanometer by eye. The beam energies were computed from the measured current drains through a permanent resistor stack leading from the kevatron ion source to ground. The values of this resistance, as a function of the current drain, had been determined by various earlier workers in this laboratory, using a cylindrical electrostatic analyzer[14] as the primary device for measuring the beam energy. The values of the stack resistance so obtained have always been reproducible to an accuracy of 1 percent.

IV. ANALYSIS OF DATA

In subtracting the zero readings to obtain the galvanometer deflections, the zeros first taken were subtracted from the pressure readings, and those obtained last were subtracted from the vacuum readings. The ratios of detector to monitor deflections under pressure and vacuum respectively were averaged to obtain $r(p)$ and $r(0)$.

The attenuation ratio, $\rho(p)$, is defined as $r(p)/r(0)$.

$$\rho(p)=\exp(-N\sigma d)=\exp(-1.930\times10^{19}pd\sigma/T), \quad (1)$$

where N is the number of gas atoms per cubic centimeter, σ is the capture or loss cross section per air atom, d is the effective path length of the particles, p is the gas pressure in mm of mercury, and T is the absolute temperature. From Eq. (1), we obtain

$$\log_{10}\rho=-0.8384\times10^{19}d\sigma p/T. \quad (2)$$

By finding the slope of the best possible straight line fitted to the experimental values of $\log_{10}\rho(p)$ *vs* p, subject to the condition that the line pass through the origin, we obtain the value of $-0.8384\times10^{19}\sigma d/T$. A least squares determination of these slopes was made, assuming that no error resided in the pressure measurements, and that the experimental values of ρ were subject to a constant probable error. Under these assumptions the probable errors in $\log\rho$ would be proportional to $1/\rho$, with the consequence that the point $(\log\rho_i, p_i)$ had to be given a weight proportional to ρ_i^2 in making the least squares fit. The formula for the slope, s, is then

$$S=\sum \rho_i^2 p_i \log\rho_i/\sum \rho_i^2 p_i^2, \quad (3)$$

and the probable error, Δ, in s is given by

$$\Delta=0.675\left\{\frac{\sum \rho_i^2(\log\rho_i)^2-s\sum \rho_i^2 p_i\log\rho_i}{(n-1)\sum \rho_i^2 p_i^2}\right\}^{\frac{1}{2}}, \quad (4)$$

where n is the number of points taken.[15]

The values of d, of course, depended on the detector used and its position. For the loss cross section, using the Montague detector at the 0° position, d was the distance from the window to the entrance slit: 12.70 cm. For the capture cross section, using the faraday cage at the 60° position, d was taken to be the length of the circular path from the window to the mouth of the faraday cage 0.5 cm behind the entrance slit, a total distance of 12.02 cm.

A typical semilogarithmic plot of $\rho(p)$ *vs* p and the best-fitting straight line to the data is given in Fig. 1.

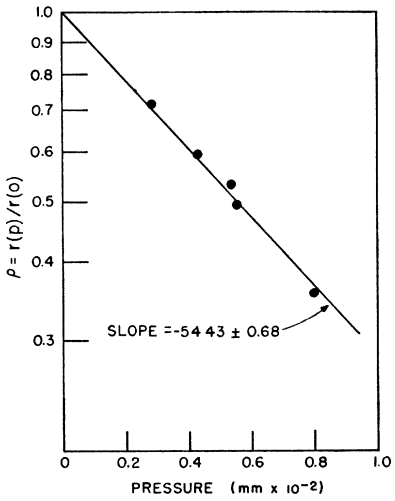

FIG. 1. Attenuation curve for a 221-kv hydrogen beam at the 0° detector.

V. SECONDARY EFFECTS

A. Effect of Gas on Detectors

Both the Montague detector and faraday cage suffered an increase in sensitivity with increasing air pressure. In the case of the Montague detector, which had a potential of 67½ volts between plates 0.32 cm apart, this effect might be ascribed to the collection of ions produced in the gas by the beam particles. The pressure dependence of the faraday cage sensitivity is not very well understood. A tentative explanation may be that, on the average, the electrons and positive ions produced a short distance in front of the faraday cage have a component of momentum in the direction toward the cage, but the exceedingly small radius of curvature of the electrons in the magnetic field present prevents their being collected.

[14] Allison, Frankel, Hall, Montague, Morrish, and Warshaw, Rev. Sci. Instr. **20**, 735 (1949).

[15] See D. Brunt, *The Combination of Observations* (Cambridge University Press, London, 1931), Chapter VI, for the theory of the probable errors of constants determined by least squares.

A measurement of the attenuation ratio with the Montague detector in the 0° position and with no magnetic field present provided a direct determination of the gas effect for this detector. The presence of gas in the chamber under conditions of no field affected the beam in two respects: (1) The ratio of charged to neutral particles entering the detector and (2) the fraction of the beam lost by simple scattering in the gas both depended on the pressure. Since the scattering cross section is strongly energy dependent, it was established that scattering effects were negligible by demonstrating that there was no reproducible dependence of the gas effect on beam energy. If the assumption that the Montague detector had equal sensitivity to charged and neutral particles is correct, the effect of gas pressure on the charge distribution of the beam does not influence this measurement. A verification of this assumption was made by repeating the gas effect

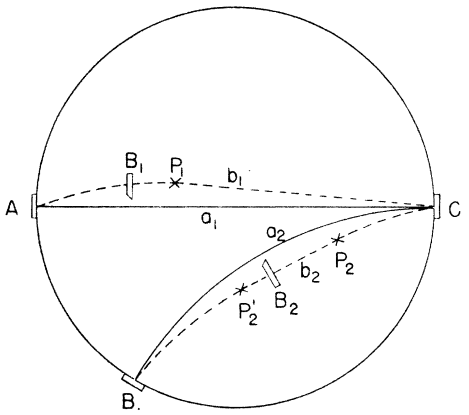

FIG. 2. Effect of scattering at the entrance window. Dotted curves depict orbits of scattered particles which would enter the detectors in the absence of baffles. A: 0° detector. B: 60° detector. C: entrance window.

measurements with a heavily aluminized zapon foil (0.1 mg/cm²) immediately in front of the detector slit. This foil was sufficiently thick that the charge distribution of the beam after penetration was independent of that of the impinging beam. No appreciable change in gas effect due to the introduction of this foil was observed.

The effect of gas on the faraday cage was measured by following the routine of a normal capture cross section measurement at such high energies ($\gtrsim 350$ kv) that the capture cross section itself was negligible. The attenuation ratios for both gas effects were, of course, greater than unity.

The data for the gas effects were treated as if they were to be considered the equivalent of negative cross sections. That is, the best slopes were found for lines through the origin representing the experimental values of $\log\rho(p)$, the slopes in this case being positive. From the slopes, equivalent negative cross sections per gas atom were deduced. The magnitude of this cross section, for the detector used, was added to the capture or loss cross section to correct for the gas effect. The values accepted were 0.54×10^{-17} cm² for the Montague detector and 0.40×10^{-17} cm² for the faraday cage, the former at the 0° and the latter at the 60° positions.

As a verification of the methods, two capture cross sections were measured, using the Montague detector instead of the faraday cage at the 60° position. Recalling that the slope of the line depicting $\log\rho$ *vs* p is divided by a factor proportional to the path length to obtain a cross section, the previously obtained gas effect cross section for the Montague detector had to be multiplied by 12.70/11.52, the ratio of the path lengths from window to detector slit in the two positions, to make it apply to the 60° position.

B. Effect of Scattering at the Window

Scattering of the incident beam by the window can cause a spurious measurement of the cross sections by processes illustrated in Fig. 2. The symbols a_1 and a_2 are the normal paths of neutral atoms and protons from the window to their respective detectors. The symbol b_1 is the path of a neutral particle which has suffered scattering in the window. If the particle loses its electron at the point P_1, it will eventually enter the 0° detector. Thus, there will be a contribution of particles to the detector, increasing with gas pressure, and therefore leading to a reduced value of the loss cross section. Similarly, b_2 represents the orbit of a scattered proton, which captures an electron at point P_2 and loses it again at P_2', these two events taking place at points such that it finally enters the 60° detector. Since this detector, the faraday cage, is sensitive only to charged particles, an electron loss process must be the final event in order that a spurious charge be detected.

Baffles B_1 and B_2 were placed in the chamber to interrupt orbits of the type just discussed. They were so placed as to miss grazing the unscattered beam by about a millimeter. Therefore, they did not completely eliminate all such orbits, leaving a residual effect that became serious only in measurements of σ_1 below 60 kv. This was evidenced by an apparent increase in the measured σ_1 with magnetic field, for the probability that a loss event can cause a scattered particle to enter the detector decreases with the radius of curvature of protons in the chamber. The experimental procedure, used in the energy range in which a dependence on magnetic field was noted, was to repeat the σ_1 measurements at increasing fields until the value of the cross section saturated. Values of σ_1 at approximately constant beam energy and varying radii of curvature are given in Table I to illustrate this saturation.[16]

No such test could be applied to the capture cross section, since the magnetic field had to be maintained at the value that would bring the unscattered proton beam to the 60° detector. However, in the case of the

[16] See Fig. 6 in reference 10 above for a graphical demonstration of this saturation.

capture cross section measurement, this effect was overshadowed by the effect of similar multiple charge exchanges in the nonscattered beam. This latter effect and the correction thereto are discussed below. No separate correction for the portion of the scattered beam not eliminated by baffle B_2 was deemed necessary.

C. Effect of Finite Detector Slit

A further correction to the loss cross section was necessitated by the failure of the Montague detector to discriminate between neutral and charged particles. If a neutral particle loses its electron when sufficiently close to the detector slit, it may still enter the detector despite the deflection caused by the magnetic field. The limiting distance from the slit for such an event is dependent on the magnetic field strength and the transverse position of the particle in the beam. By averaging this distance over the breadth of the beam, Montague[10] derived the approximate relationship,

$$b=\tfrac{2}{3}(2Rw)^{\frac{1}{2}}, \tag{5}$$

where b is the average distance in front of the slit for detection despite electron loss, R is the radius of curvature of a proton in the magnetic field present, and w is the slit width. Thus the effective path length from window to detector is reduced to $d-b$. The correction factor to be applied to the loss cross section is

$$1+(2/3d)(2Rw)^{\frac{1}{2}}=1+0.0237\,R^{\frac{1}{2}}, \tag{6}$$

an eight percent correction for the 11-cm radius of curvature usually used.

D. Correction of δ_c for the Effect of Multiple Charge Exchanges

At energy values at which $\sigma_1>3\sigma_c$, a departure from linearity was observed in the plots of $\log\rho$ against pressure, the departure being in the direction of too low values for $|\log\rho|$. This was ascribed to the effect of multiple processes of the following type: A proton captures an electron, travels in a straight line a distance δ, loses the electron again, and continues in a circular orbit equivalent to the initial one displaced a vector distance δ. If δ is less than a limiting value dependent on the position of the proton at the time of the capture, the ultimate orbit will still terminate within the detector entrance slit.

An approximate quantitative treatment of this effect has been attempted. The coordinates used are illustrated in Fig. 3. The letter x is the arc length along the bent beam, measured from the window; y is the transverse coordinate, measured from the outer periphery of the beam arc; and θ is the angular coordinate about the center of curvature of the beam, measured from the detector slit. The shaded area represents the portion of the beam that would normally enter the detector slit. The total beam has a somewhat greater width, equal to that of the collimating apertures. Only half of this excess width, shown as the nonshaded area in the figure, is pertinent to the treatment at hand.

TABLE I. Saturation of loss cross section with decreasing radius of curvature.

Beam energy E (kv)	Loss cross section σ_1 (cm$^2\times10^{-17}$)	Radius of curvature R (cm)
34.3	16.45±0.36	11.0
41.4	20.35±0.14	5.84
40.8	23.28±0.47	3.88
41.4	22.21±0.63	3.30

If a proton becomes neutral at a point (x, y) with $y<w$, the slit width, it will still enter the detector provided it loses the electron again before it has travelled a distance greater than $y/\sin\theta$. Particles in the region $y>w$, normally never entering the detector, will be detected if, after capturing an electron, they travel a distance between $(y-w)/\sin\theta$ and $y/\sin\theta$ before they lose it again.

We can then write the differential equation,

$$dn=nN\sigma_c dx\left\{\int_{0.107}^{0.136}\frac{dy}{0.107}\left[e^{-(y-0.107)N\sigma_1/\sin\theta}-e^{-yN\sigma_1/\sin\theta}\right]-\int_0^{0.107}\frac{dy}{0.107}e^{-yN\sigma_1/\sin\theta}\right\}, \tag{7}$$

where the slit width, w, is 0.107 cm; the total beam width considered is 0.136 cm; n is the flux of protons at position x; N is the number of gas atoms per cm^3; and σ_c and σ_1 are the electron capture and loss cross sections, respectively. The total arc length from window to slit is 11.52 cm and the radius of curvature of the beam is 11.0 cm. Hence θ will equal $(1/11)(11.52-x)$ radians.

For small values of θ, the above formulation becomes inaccurate. From Eq. (5) above, the average distance in front of the slit from which particles will enter the detector regardless of their charge state is 1.02 cm. Moreover, the mouth of the faraday cage was 0.5 cm behind the slit. Hence Eq. (7) was integrated to $x=10.5$ cm, and the flux entering the cage was obtained by multiplying the flux at 10.5 cm by the factor

$$[\sigma_c e^{-1.52N(\sigma_c+\sigma_1)}+\sigma_1]/(\sigma_c+\sigma_1).$$

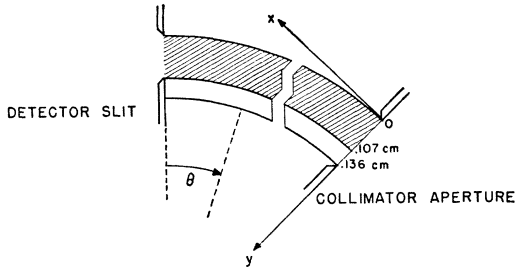

FIG. 3. The coordinates used in discussing the correction for multiple charge exchanges.

TABLE II. Result of numerical evaluation of $\int_0^{10.5} I(N\sigma_l, x)dx$ as a function of $N\sigma_1$.

$N\sigma_l$ (cm^{-1})	$\int_0^{10.5} I dx$
0.1	0.1100
0.2	0.2152
0.3	0.3160
0.4	0.4128
0.5	0.5053
0.6	0.5943
0.7	0.6797
0.8	0.7617
0.9	0.8404
1.0	0.9160
1.1	0.9889

Then the attenuation ratio, ρ, will be given by

$$\log_{10}\rho_1=\frac{-0.4343\sigma_c}{0.107\sigma_l}\int_0^{10.5} I(N\sigma_l, x)dx + \log_{10}\left\{\frac{\sigma_c e^{-1.52N(\sigma_c+\sigma_l)}+\sigma_l}{\sigma_c+\sigma_l}\right\}, \quad (8)$$

where

$$I\equiv \sin\theta e^{-0.029N\sigma_l/\sin\theta}[1-e^{-0.107N\sigma_l/\sin\theta}]. \quad (9)$$

The integration over x has been carried out numerically for a number of values of $N\sigma_l$, and the results listed in Table II. Figure 4 illustrates σ_l/σ_c times the predominant first term of Eq. (8) plotted against $N\sigma_1$, as compared to the line

$$(\sigma_l/\sigma_c)\log_{10}\rho(10.5\text{ cm})=-0.4343N\sigma_l\times 10.5,$$

where $\rho(10.5$ cm$)$ would be the attenuation ratio at $x=10.5$ cm, were multiple processes not present. The pressure is to be considered the varying parameter in $N\sigma_l$.

This derivation of the attenuation ratio clearly overestimates the effect of multiple processes, since it ignores the fact that a particle which has suffered a double charge exchange, and yet is in an orbit that will enter the detector, will also suffer a displacement of its orbit

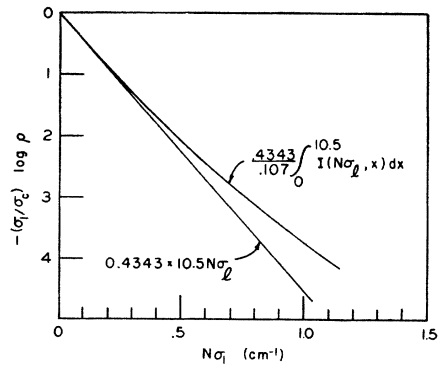

FIG. 4. The predominant term in $(\sigma_l/\sigma_c)\log\rho$ after consideration of the effect of multiple charge exchanges. The straight line represents the expected value of $(\sigma_l/\sigma_c)\log\rho$ in the absence of this effect.

toward lower y-values. Loss from the beam following a subsequent capture process will then be more probable.

An alternate treatment, which will underestimate the multiple process effect, is carried out by assuming a flux at x of strength $\exp(-N\sigma_c x)$ and considering the flux increment due to double processes as a perturbation. Then the contribution from double processes in dx at x will be given by

$$N\sigma_c dx\exp(-N\sigma_c x)[1-(1/0.107N\sigma_l)I(N\sigma_l, x)].$$

This contribution is assumed to decay by the factor $\exp[-N\sigma_c(10.5-x)]$, leaving a net contribution at $x=10.5$ cm of

$$N\sigma_c dx\exp(-10.5N\sigma_c)[1-(1/0.107N\sigma_l)I(N\sigma_l, x)].$$

Integrating this contribution over x, adding it to the unperturbed flux, and multiplying by the factor for the attenuation in the final 1.52 cm of the path, we have

$$\rho_2=e^{-10.5N\sigma_c}\left\{(1+10.5N\sigma_c) - \frac{\sigma_c}{0.107\sigma_l}\int_0^{10.5} I(N\sigma_l, x)dx\right\}\frac{\sigma_c e^{-1.52N(\sigma_c+\sigma_l)}+\sigma_l}{\sigma_c+\sigma_l}. \quad (10)$$

It can be easily shown that

$$\log_{10}\rho_2-\log_{10}\rho_1<0.2172\left[10.5N\sigma_c - (\sigma_c/0.107\sigma_l)\int_0^{10.5} I(N\sigma_l, x)dx\right]^2. \quad (11)$$

That Eq. (10) underestimates the multiple process effect is shown by the fact that the double process contribution taken is too small, since the true flux is greater than $\exp(-N\sigma_c x)$. Furthermore this contribution then decays less than $\exp[-N\sigma_c(10.5-x)]$, since it can undergo further double processes without being lost to the detector.

Defining $\log\bar{\rho}$ as the arithmetic mean of $\log\rho_1$ and $\log\rho_2$, and f as $12.02\times 0.4343N\sigma_c/(-\log\bar{\rho})$, we can correct the observed values of $\log\rho$ by multiplication by f. Table III lists $-\log\rho_1$, $-\log\rho_2$, $12.02\times 0.4343N\sigma_c$, and f *vs* $N\sigma_l$ for a typical case, in which $\sigma_c=3.24\times 10^{-17}$ cm^2 and $\sigma_l=21\times 10^{-17}$ cm^2. Figure 5 illustrates a typical set of capture points before and after this correction.

As can be seen from the illustration, this correction becomes significant only at pressures such that $N\sigma_l>0.2$ cm^{-1}. Hence, the departure from linearity was only noticed when $\sigma_c<13\times 10^{-17}$ cm^2, for only then were relatively high pressures ($p>10^{-2}$ mm) admitted to the chamber. Furthermore, the effect did not show up in Ribe's work, for the loss cross section in hydrogen is a factor of four smaller, and the highest pressure he used was 7×10^{-2} mm (limit of the McLeod gauge). Hence his highest value of $N\sigma_l$ was only 0.18 cm^{-1}.

E. Effect of Formation of H^- Ions

The possibility of the formation of negative hydrogen ions raises the question of whether the measured loss cross section is not in part the cross section for capture of an electron by a neutral hydrogen atom, a process which would also contribute to the attenuation of a neutral beam. While a complete answer cannot now be given to this question, a measurement has been made which leads to some estimate of the possibilities. The ratio of negative ions to protons leaving the window was found by Ribe[11] to be 0.026 at 35 kv, and less than 0.001 at 90 kv. This value was obtained by comparing the galvanometer deflections from the faraday cage at 60° for the two components, the magnetic field being reversed to bring the negative ions to the detector. If it is assumed that the window was of a thickness yielding charge equilibrium, the ratio of negative ions

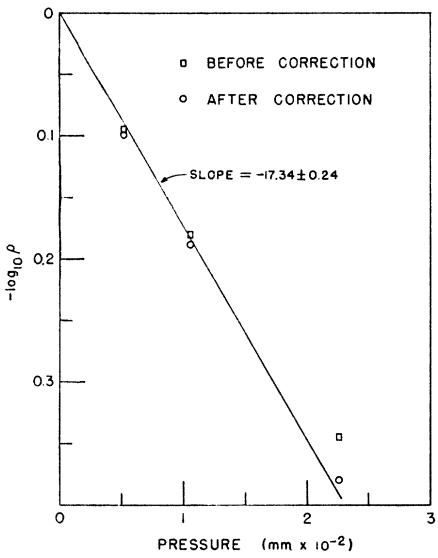

FIG. 5. Attenuation curve for a 93-kv proton beam at the 60° detector before and after correction for multiple charge exchanges.

to protons equals $\sigma_c\sigma_c^*/\sigma_l\sigma_l^*$, where σ_c and σ_l are defined as before, σ_c^* is the cross section for electron capture by a neutral atom, and σ_l^* is the cross section for electron loss by a negative ion. Then, at 35 kv

$$\sigma_c^*=0.026\sigma_l\sigma_l^*/\sigma_c>0.026\sigma_l^2/\sigma_c, \qquad (12)$$

since σ_l^* is certainly greater than σ_l. Assuming the same σ_l and σ_c for the window material as for air, this leads to $\sigma_c^*>0.77\times10^{-17}$ cm² at 35 kv, which is to be compared to an extrapolated value for σ_l of 23.5×10^{-17} cm². A crude upper limit to σ_c^* may be set by assuming that the collision radius for electron loss by an H^- ion is not greater than the sum of the radii of an H^- ion and an air atom. In a compilation by Wherry[17] of

[17] E. T. Wherry, Am. Mineral. **14**, 54 (1929). The tabulation given is based on a set of wave-mechanical values computed by Pauling (J. Am. Chem. Soc. **49**, 765, 1927), and values computed by V. M. Goldschmidt *et al.* on the basis of empirical assumptions (Geochemische Verteilungsgesetze der Elemente: VII. "Die Gesetze der Krystallochemie"; Skrifter Norske Videnskaps-Akad. Oslo. I. Mat.-Natur. Kl., No. 2, 1926). Pauling's value is used for H^-, and Goldschmidt's for N and O.

TABLE III. Dependence of $\log_{10}\rho_1$, $\log_{10}\rho_2$, $(0.4343)(12.02)N\sigma_c$, and f on $N\sigma_l$ for the case $\sigma_c=3.24\times10^{-17}$ cm², $\sigma_l=21\times10^{-17}$ cm². The parameter $N\sigma_l$ equals $13.72p$, where p is the pressure in mm of mercury.

$N\sigma_l$	$-\log_{10}\rho_1$	$-\log_{10}\rho_2$	$0.4343\times12.02N\sigma_c$	f
0.1	0.0684	0.0683	0.0706	1.032
0.2	0.1324	0.1324	0.1412	1.066
0.3	0.1927	0.1927	0.2118	1.100
0.4	0.2496	0.2497	0.2824	1.132
0.5	0.3034	0.3034	0.3530	1.166
0.6	0.3550	0.3547	0.4236	1.199
0.7	0.4042	0.4038	0.4942	1.231
0.8	0.4521	0.4512	0.5648	1.262
0.9	0.4987	0.4969	0.6354	1.294
1.0	0.5444	0.5413	0.7060	1.324
1.1	0.5901	0.5850	0.7766	1.353

accepted values of atomic radii, 0.71×10^{-8} cm and 0.60×10^{-8} cm are given for the neutral nitrogen and oxygen atoms, respectively; and 2.08×10^{-8} cm is given for the negative hydrogen ion. Using the value for nitrogen, an upper limit of 24.4×10^{-16} cm² is obtained for σ_l^*, leading to upper limits for σ_c^* of 8×10^{-17} cm² at 35 kv and 1×10^{-17} cm² at 90 kv.

VI. RESULTS

The final values of σ_l and σ_c are listed in Table IV and also plotted in Fig. 6. The two points labelled "*M*" on the σ_c curve were taken with the Montague detector at the 60° position. In the energy range shown, σ_l and σ_c are well represented by the following empirical formulas:

$$\sigma_l=(24.54-0.866E/E_0)\times10^{-17}\text{ cm}^2, \qquad (13)$$

$$\sigma_c=[41.1\exp(-0.562E/E_0)]\times10^{-17}\text{ cm}^2, \qquad (14)$$

where $E_0=24.8$ kv, the kinetic energy of a proton

TABLE IV. The electron capture and loss cross sections for hydrogen beams passing through air.

Beam energy E (kv)	Electron-loss cross section per atom σ_l (cm² $\times10^{-17}$)	Beam energy E (kv)	Electron-capture cross section per atom σ_c (cm² $\times10^{-17}$)
40.8	24.37±0.47	31.4	20.80±0.37
41.4	23.17±0.63	38.2	17.65±0.21
67.0	22.22±0.06	40.6	15.97±0.46
105	20.84±0.25	43.0	15.64±0.30
107	21.00±0.30	49.4	13.39±0.36
117	20.63±0.11	55.7	11.59±0.23
142	19.76±0.10	56.6	11.51±0.22
156	18.88±0.06	58.1	10.07±0.14
193	17.35±0.35	63.0	9.74±0.21
221	16.74±0.19	65.6	9.26±0.19
252	14.42±0.72	73	6.80±0.29
280	14.53±0.30	77	7.06±0.18
325	13.58±0.25	93	5.52±0.07
...	...	114	3.38±0.04
...	...	117	2.72±0.07
...	...	122	2.70±0.04

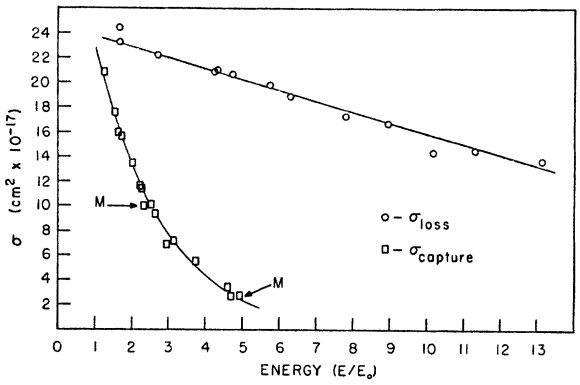

FIG. 6. Electron capture and loss cross sections as functions of ion energy for hydrogen beams in air. $E_0=24.8$ kv, the kinetic energy of a proton moving with the Bohr velocity.

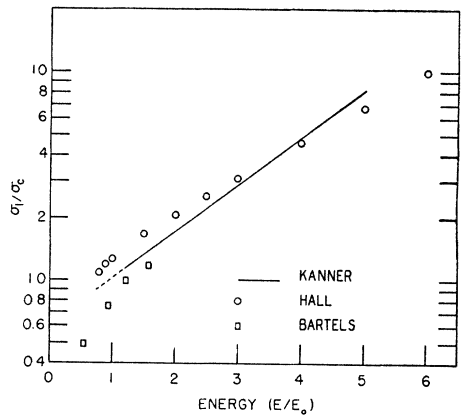

FIG. 7. The ratio of loss to capture cross sections as a function of ion energy. The solid curve is a plot of σ_l/σ_c as given by Eqs. (13) and (14). Bartels' points are for hydrogen beams in air, and Hall's points for hydrogen beams in the metals Be and Ag.

moving with velocity $v_0=e^2/\hbar$. σ_l/σ_c as given by Eqs. (13) and (14) is plotted in Fig. 7, which also shows the values obtained by Bartels[3] for air and by Hall[9] for metals. Both the capture and loss cross sections decrease considerably less steeply with increasing energy than has been predicted theoretically by Bohr,[18] who gives a dependence proportional to $E^{-\frac{1}{2}}$ for the loss cross section, and proportional to E^{-3} for the capture cross section. Since both of Bohr's formulas require $v\gg v_0$, (say $v\sim 6v_0$) this disagreement in the energy range of the present investigation is not surprising.

VII. DISCUSSION OF ERRORS

The uncertainties listed in Table IV as accompanying the cross sections are derived purely from the scattering of the $\rho(p)$ values about the chosen straight line by application of Eq. (4). They therefore take into account random errors during a measurement, such as those originating in faulty instrument reading, amplifier drift, and beam inhomogeneity.

The accuracy of the energy measurements is greater for the capture cross section than for the loss cross section, a fortunate circumstance in view of the steeper energy dependence of the former. The system of collimator, magnetic field, and 60° detector slit acted as a magnetic spectrometer, so that the outstanding uncertainty in the energy for a σ_c measurement was due to the probable 1 percent error in the magnet calibration. In the case of the σ_l measurements, the additional uncertainty because of straggling in the entrance window and ripple in the kevatron voltage was present. Of the two, the 3 percent ripple overshadowed the contribution of the straggling to the energy uncertainty.

The McLeod gauge used for the pressure measurements had been calibrated by Ribe and the author by measuring the volume of the bulb and the bore of the capillary. This calibration is considered to be correct to better than 1 percent.

The measured gas effects on the detectors are believed correct to within an equivalent cross section of 0.2×10^{-17} cm², thus introducing maximum errors in the cross sections of 1.5 percent in the value of σ_l at 325 kv and 8 percent in σ_c at 125 kv.

[18] N. Bohr, Kgl. Danske Videnskab. Selskab. Mat.-fys. Medd. (1948), Equations 4.2.8 and 4.3.5.

VIII. ACKNOWLEDGMENTS

The author wishes to express his gratitude to Dr. S. K. Allison for suggesting the problem and extending the facilities of his laboratory. Thanks are also due Dr. F. L. Ribe, Mr. D. S. Bushnell, and Mrs. L. C. Kanner for their aid in taking the many data. Finally, the author wishes to thank Mr. H. Casson and Mr. J. Alexander for their valuable participation in discussions of the correction for multiple charge exchanges.